RESIN TREATMENT OF FREE EDGES TO AID CERTIFICATION OF THROUGH THICKNESS LAMINATE STRENGTH

Timothy A. Fletcher[a]*, Tatiana Kim[b], Timothy J. Dodwell[c],
Richard Butler[d], Robert Scheichl[e], Richard Newley[f]

[a,b,d,f] Department of Mechanical Engineering, University of Bath,
Claverton Down, Bath BA2 7AY, United Kingdom

[c] College of Mathematics, Engineering and Physical Sciences,
University of Exeter, Exeter, EX4 4PY, United Kingdom

[e] Department of Mathematical Sciences, University of Bath,
Claverton Down, Bath BA2 7AY, United Kingdom

[a] t.a.fletcher@bath.ac.uk [b] t.kim@bath.ac.uk [c] t.dodwell@exeter.ac.uk
[d] r.butler@bath.ac.uk [e] r.scheichl@bath.ac.uk [f] rn379@bath.ac.uk

ABSTRACT

Large aerospace parts are typically certified by testing narrow specimens, such as curved laminates, which have exposed free edges. These edges (not present in the production part) have been found to reduce the 3D strength of curved laminates by over 20%, showing this certification method is unreasonably conservative. The free edges also create a singularity, such that Finite Element (FE) modelling is challenging, which is typically approximated using non-linear analysis of cohesive interlaminar zones. A new treatment process is developed whereby a layer of resin is applied to the free edges of curved laminates. This significantly reduces the edge effect and delays failure. The resin edge treatment increases the strength of the curved laminate test specimens by 16%. The treatment also simplifies FE modelling by allowing for non-zero stresses normal to the laminate edge, removing the singularity. This enables use of linear FE models, which converge at the laminate edge. A linear FE method developed in this paper is conservative and predicts the strength of treated curved laminates to within 5% of the average test value. Hence it is shown that the resin edge treatment can be used to improve reliability of both certification tests and FE models.

Keywords: Curved laminates; 4-point bending; Free edge; Edge effect.

*Corresponding author

NOMENCLATURE

Abbreviations

CBS	=	Curved beam strength – required moment per unit width for failure.
CFRP	=	Carbon fibre reinforced plastic.
FE	=	Finite Element.
FEA	=	Finite Element Analysis.
ILSS	=	Interlaminar shear strength.
LHS	=	Left hand side.
UD	=	Uni-directional.
UTS	=	Ultimate tensile strength.

Symbols

D	=	Roller diameter.
d_x	=	Horizontal distance between centre of adjacent upper and lower roller.
d_y	=	Vertical distance between centre of adjacent upper and lower roller.
i, j	=	Local directional parameters with 1 and 2 in-plane and 3 out-of-plane.
P	=	Applied load.
Φ	=	Angle between limbs of curved laminate and horizontal.
s_{ii}, s_{ij}	=	Material allowable.
σ_{ii}	=	Direct stress.
t	=	Thickness of curved laminate.
τ_{ij}	=	Shear stress.
w	=	Width of curved laminate.

1 INTRODUCTION

The certification of aircraft is typically validated with a programme of testing. Thousands of tests are carried out on small scale coupons, with fewer and fewer carried out as the test parts get larger and more complex. It is important that at every scale the test is representative of the final product. The response of curved laminates to out-of-plane loading can be assessed by conducting a 4-point bend test [1]. These tests are typically carried out on small curved laminate specimens, several orders of magnitude narrower than the final product. For UD CFRP material, considered in this paper, bending tests induce high interlaminar stresses at the free edges of such narrow specimens, generated by the mismatch in elastic properties between plies with different fibre orientations. This edge-effect generally causes narrow specimens to fail at a significantly lower load than would be predicted by 2D, plane strain analysis. It therefore results in the narrow specimen not being representative of the final

product, where the final product is very wide and/or is built into surrounding structure at its ends, such that it has no free edges.

The high stress intensity caused by free edges has long been a known issue and there have been many techniques proposed to reduce it. Caps can be bonded onto the free edges and this has been shown to reduce interlaminar normal stress but does not significantly reduce interlaminar shear stress [2-5]. The edges can be altered to tailor structural properties, using an isotropic filler material and by changing the orientation of a ply near the free edge to reduce interlaminar stresses in this region [6]. A number of other techniques have been used to mitigate the free edge effect, such as stitching along the edges [7] and the use of adhesive layers [8]. It has also been shown that the stacking sequence of the laminate is important and can be tailored to influence the interlaminar stresses near a free edge [9]. The vast majority of edge protection techniques have been applied only to flat laminates under axial loading.

Evaluating the edge effect is challenging and many analytical and numerical approximation methods have been proposed. Literature surveys of these can be found in review articles [10-11] but there are no analytical methods that calculate the exact stresses at the free edge. An approximate analytical method for calculation the interlaminar stresses for laminated plates is presented in [12]. This work shows the singular behaviour of interlaminar normal and shear stresses near laminate free edges, which gives rise to the challenges and complexity in modelling such problems. Linear FE analysis often results in highly localised, mesh dependent stresses near the edge that are higher than the strength of the material. A method for assessing when these high stresses will lead to failure has been developed using linear elastic fracture mechanics [13]. Non-linear FE analysis of cohesive zones is often performed in order to capture failure initiation and predict composite laminate strength, such as 3D non-linear modelling of delamination damage onset and growth in composite spar wingskin joints [14]. 3D non-linear FE modelling is generally very computationally expensive. An alternative

method for assessing the free edge effect for composite flat plates is described in [15]. This consists of assessing 2D and 1D problems through a series of iterations, which produces quasi-3D results less costly than full 3D FEM computations.

In this paper a number of 4-point bend tests have been carried out alongside linear FE analysis to investigate the strength of curved laminates. In this way the edge effect is established as well as the convergence of the FE models. Thereafter a resin edge treatment designed to protect the free edges is developed and explored in order to reduce the edge effect. The treatment consists of a band of resin applied to the free edges of the laminate. A diagram of the curved laminates is shown in Fig. 1, illustrating the free edges and resin edge treatment. It has been shown that reducing the fibre volume fraction towards the free edge reduces interlaminar stresses for a flat laminate under axial extension [16]. The technique presented in this paper has some similarities to this, with effectively a fibre volume fraction of zero within the resin edge treatment zone. However, a key benefit of the new treatment is that it can be applied retrospectively to samples cut from larger parts.

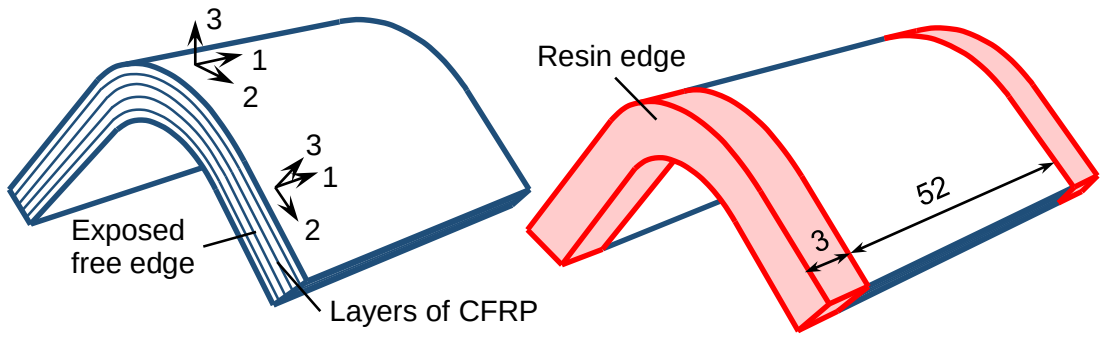

Figure 1 Curved laminates without and with resin edge treatment, showing the free edge in the untreated sample and how this is protected by resin for the treated sample. The axes show the global coordinate system. Fibres in 0° plies are oriented along the 1-axis and 90° plies, along the 2-axis. Dimensions in mm, not to scale.

2 TEST METHODOLOGY

2.1 Rig Design and CBS Calculation

The curved beam strength (CBS) is used as a metric for quantitatively assessing and comparing the strength of the curved laminates. CBS is defined as the applied bending moment per unit width (or running moment) at failure. The CBS of curved laminate specimens was assessed by means of a 4-point bend test. The test setup was adapted from ASTM D6415 [1]. An unfolding moment was generated by 4 rollers attached to a test rig, as shown schematically in Fig. 2.

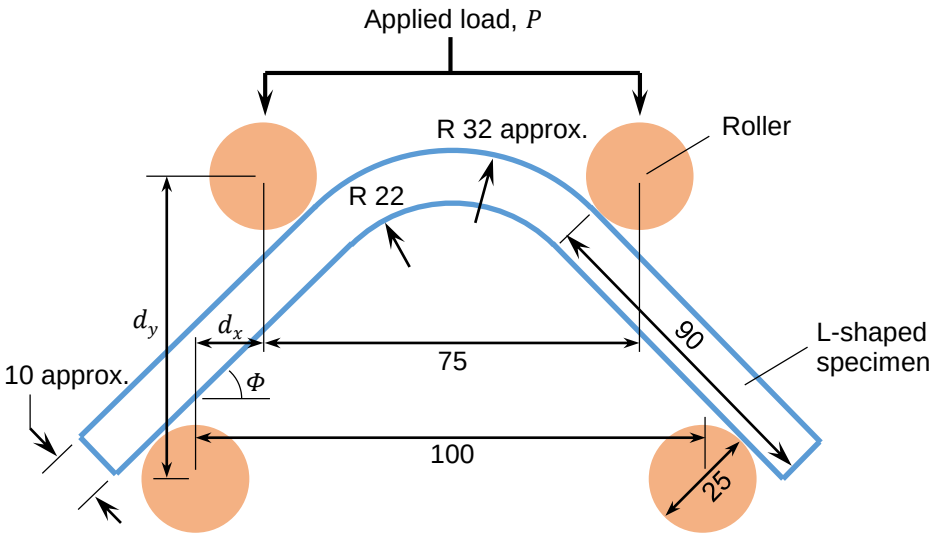

Figure 2 Schematic of test setup in cross-section. All dimensions in mm.

Well-lubricated, smooth steel rollers were used in order to ensure they rotated freely within their housing and could not transfer load into the coupon via shear, which would invalidate many of the modelling assumptions. The displacement of the upper two rollers was controlled by an Instron machine at a rate of 1 mm/min. By monitoring the load and displacement, the applied moment, and hence CBS, was calculated from [1] according to

$$CBS = \left(\frac{P}{2w\cos\Phi}\right)\left(\frac{d_x}{\cos\Phi} + (D+t)\tan\Phi\right) \quad (1)$$

$$\sin\Phi = \frac{-d_x(D+t) + d_y\sqrt{{d_x}^2 + {d_y}^2 - D^2 - 2Dt - t^2}}{{d_x}^2 + {d_y}^2} \quad , \quad (2)$$

where w and t are, respectively, the width and thickness of the specimen and D is the roller diameter. All other parameters are defined according to Fig. 2. Note that d_y and hence Φ changes during the test as the upper rollers displace downwards. The values at failure were taken to calculate CBS. The selection of d_x was as small as possible to minimise vertical displacement to failure (and hence geometrical non-linearity), without being so small as to induce failure by shear in the limbs.

2.2 Specimen Preparation

A large C-section structure was manufactured from M21/IMA uni-directional CFRP material. Using an AFP machine, 39 plies were laid up, with final cure in an autoclave. The nominal ply thickness was 0.25 mm, giving a total laminate thickness of approximately 10 mm post-cure. The laminate consisted of the symmetric sequence of fibre angles $[(\mp45/90/0)_2/\mp45_2/90/\mp45/90/0/\mp45/0/\pm45/0/90/\pm45/90/\pm45_2/(0/90/\pm45)_2]$, where 90° fibres wrap around the corner, along the axis labelled 2 in Fig. 1. Curved laminate specimens were then cut from the C-section according to the dimensions in Fig. 2, with a nominal width of 52 mm. The free edges were then finely polished to avoid exacerbating the edge effect and the final width was measured after the final grinding process was complete.

2.3 Resin Edge Treatment

Treatment was applied to the free edges of a number of the specimens. After the edges had been polished they were plasma treated, in order to ensure the highest quality bond possible, and then the resin (EP1330LV, supplied by Resinlab) was applied. A mould was used to

control the shape of the resin edge, such that it was prismatic with the curved laminate (see Fig. 1). Resin was poured into the mould by hand and cured in an oven before being ground back so that approximately 3 mm of resin was left on each free edge, increasing the overall specimen width to approximately 58 mm, as shown in Fig. 1. However, for the purposes of calculating CBS according to Eq. (1), the width was taken as that of the CFRP only. At a laminate free edge there is an infinite contrast in mechanical properties across the free edge. The resin edge treatment works by reducing this contrast. Since CFRP is generally much stiffer than pure resin, is it important that a high modulus resin is used to minimise the contrast across the CFRP-resin edge boundary. The effect of resin modulus is discussed in section 6.3.

3 TEST RESULTS

Each test was stopped immediately after the first failure event occurred, identified by either an audible crack or load drop. The specimen was then inspected visually, using a microscope and CT scanner to identify the location of first failure. A summary of the test results is shown in Table 1.

Sample	Edge treatment	CBS (kNmm/mm)	Average CBS
A-1	None	7.56	7.49
A-2	None	7.19	
A-3	None	7.71	
B-1	Resin	8.70	8.65
B-2	Resin	8.60	
B-3	Resin	8.66	

Table 1 Test results for curved laminate specimens without and with resin edge treatment, showing an increase in CBS of 16% for the average test result of the treated specimens.

From Table 1 it can be seen that the specimens that had resin edge treatment consistently achieved a higher CBS than those without treatment, with average CBS increase of 16%. The failure location of the test specimens was found to be relatively predictable, with a clear

difference between specimens that were resin edge treated and those that were not. The specimens generally failed with multiple delaminations simultaneously (see Fig. 3 and Fig. 4), meaning it was not possible to determine where failure first occurred from test data alone. However, the untreated specimens all failed within the inner half of the laminate only. Figure 3 shows Sample A-1 but A-2 and A-3 also failed in a very similar manner. In contrast, the edge treated specimens all exhibited large delaminations throughout the thickness of the laminate, as shown in Fig. 4a. At the point of failure during the test, the resin edge shattered, leaving the free edge of the CFRP exposed, as shown in Fig. 4b. Figure 4 shows Sample B-1 as an example but B-2 and B-3 also exhibited similar failure behaviour.

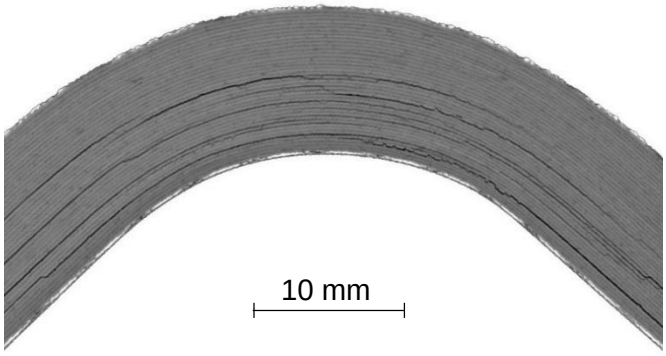

Figure 3 Post-test CT scan cross-section of Sample A-1, without resin edge treatment. Failure locations are within the inner half of the laminate only (towards the inner radius).

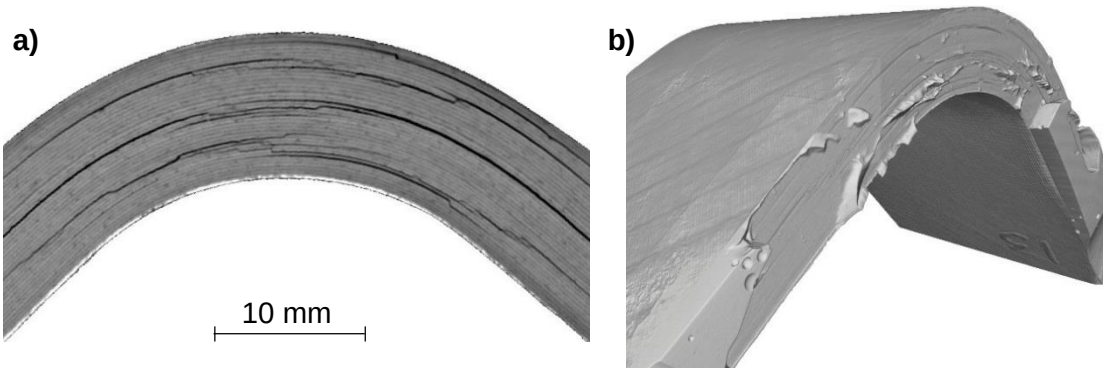

Figure 4 Post-test CT scan of Sample B-1, with resin edge treatment. **a)** Cross-section within the CFRP. Failure locations are seen throughout the laminate thickness, in contrast with the untreated specimen. **b)** Isometric view showing damage to the resin edge, which has mostly broken away from the CFRP edge at the point of failure. The remaining fragments are visible.

4 FINITE ELEMENT MODELLING

Finite Element modelling was conducted using ABAQUS software [17]. In the model, the curved laminates were assumed to have the nominal width of 52 mm. The plies were assumed to have a thickness of 0.24 mm, with a 0.015 mm interface layer of pure resin between each ply. This is primarily based upon measurements taken from micrograph images of the curved laminates, see for example Fig. 5. There is not a clear boundary between ply and interface, which means there is an element of subjectivity when measuring thickness, of the interface layer in particular. An interface thickness of 0.019 mm has been measured for a similar material (M21/T700) [18]. A sensitivity analysis is presented in section 6.1 to address the uncertainty regarding ply and interface thickness.

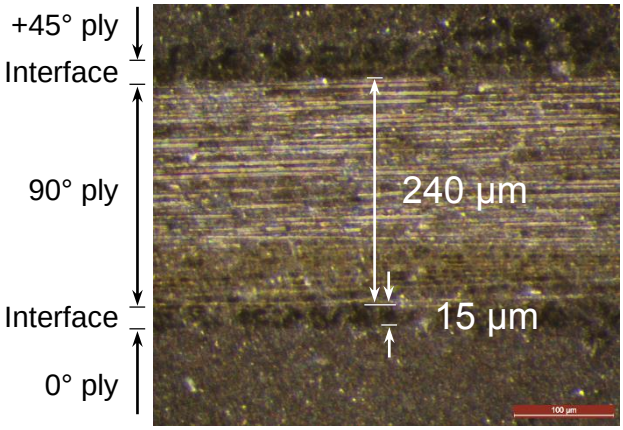

Figure 5 Micrograph showing layers of CFRP with thickness measurement of ply and interface (resin rich layer between plies).

The assumed mechanical properties for both the fibrous ply material and the resin rich interface material are given in Table 2. E_{11} was found by averaging tension modulus and compression modulus, which are quoted in the Hexcel datasheet for M21/IMA [19]. E_{22} and E_{33} values for M21/IMA are not quoted, however for 8552/AS4 [20] the 90° tensile modulus is given as 10 GPa and M21 is derived from the resin system 8552. Also, a dynamic characterisation of M21/T700GC [21] found values for E_{22} ranging between 10.10 - 10.56 GPa. Although this is a different fibre, the resin will dominate E_{22} and E_{33}, such that similar values can be expected

for M21/IMA. G_{13} is assumed equal to the in-plane shear modulus, G_{12} [19]. G_{23} and Poisson's ratio values were not found so values typically found in similar CFRP systems were taken. The through-thickness shear strength, s_{13}, was assumed equal to the ILSS [19]. The through-thickness tensile strength, s_{33}, is not directly quoted for M21/IMA, however for 8552/AS4 the 90° tensile strength and ILSS are quoted as 81 and 128 GPa respectively [20]. Assuming the same ratio between s_{33} and s_{13} for M21/IMA as for 8552/AS4 gives $s_{33} \approx 61$ GPa. The assumed properties for the resin edge material of the treated curved laminates are also shown in Table 2 [22].

Orthotropic fibrous layer		**Isotropic interface layer**			**Resin edge material**	
E_{11}	162 GPa	E	10 GPa		E	8.5 GPa
E_{22}, E_{33}	10 GPa	v	0.35		v	0.35
G_{12}, G_{13}	5.2 GPa					
G_{23}	3.5 GPa	**M21/IMA allowables**			**Resin edge allowable**	
v_{12}, v_{13}	0.35	s_{33}	61 MPa		UTS	55 MPa
v_{23}	0.5	s_{13}	97 MPa			

Table 2 Assumed mechanical properties for resin edge material (EP1330LV) and CFRP material (M21/IMA), where 1 is the fibre direction in-plane, 2 is perpendicular to the fibre direction in-plane and 3 is out-of-plane. s_{33} is the tensile through-thickness strength and s_{13} is the transverse shear strength.

Modelling the full 3D bending test with rollers (illustrated in Fig. 2) and contact analysis would be extremely computationally expensive and restrict mesh fidelity. Therefore a simplified model was used. Curved laminates were modelled with shortened limbs; of length 10 mm, approximately equal to the thickness of the laminate. A moment was applied to the end of one limb using a beam multi-point constraint (MPC), with all degrees of freedom fixed at the end of the opposite limb. Figure 6 illustrates this in 2D for clarity, however the model used was 3D. Whilst this does not accurately model stresses in the limbs, it gives the same stress field towards the apex of the curved section as a full model with rollers. In this region there is a pure moment (without shear) caused by the roller displacement. Since this is the critical region where failure occurs during the tests, this implies the simplified model is suitable for predicting CBS.

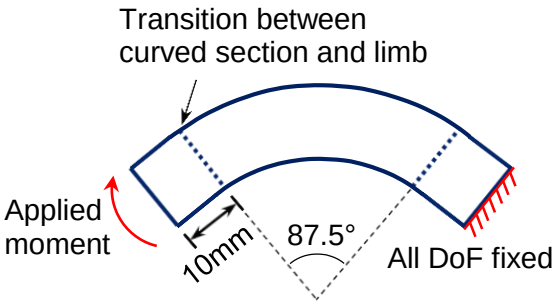

Figure 6 Schematic of FE model shown in 2D for clarity, although the model used is 3D. Only a small section of the limbs is modelled with one fixed and a moment applied to the other to simulate the effect of the roller displacement during the test.

4.1 Mesh Refinement and Model Parameters

Standard linear hexahedral elements are used throughout the model with reduced integration (ABAQUS element C3D8R). Stresses change most rapidly in the vicinity of the free edge and this is also the key area of interest for failure initiation. Therefore, the FE mesh is graded, such that there is higher fidelity near the edge than towards the mid-width, which has been shown to significantly reduce modelling errors [23]. The fibrous layers are modelled with 6 elements through thickness, graded such that the outer elements are smaller than those in the middle of the layers. Modelling undertaken in [23] produced satisfactory results with 5 elements per layer (through thickness), also with element size near the interface reduced. The interface layers are modelled with 2 elements through thickness, which is believed sufficient since bending of the interface layers is not important to the modelling. Around the curved section there are 50 equally sized elements (no grading) and down each limb 5 equally sized elements (no grading). The grading (across the laminate width and through thickness) is achieved using the double bias option in the mesh seeding tool of ABAQUS, which produces a finer mesh towards either end of the line being seeded. The number of elements along a line is set, together with the bias ratio, which determines the approximate ratio between the smallest and largest element. An example of this is illustrated in Fig. 7. A summary of all the mesh seeding is contained within Table 3.

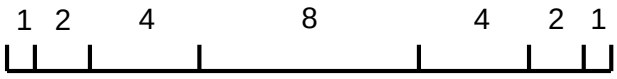

Figure 7 Line separated into 7 elements with double bias ratio of 8, meaning the middle element is 8 times larger than the outer most elements, with adjacent elements scaling by a factor or 2.

		No. elements	Bias ratio
Across width		40	1000
Through thickness	Fibrous layer	6	3
	Interface layer	2	-
Around curved section		50	-
Down each limb		5	-

Table 3 Summary of mesh seeding for FE model of curved laminate. Note that the number of elements and bias ratio across the width was varied as part of reliability and singularity studies in 5.1.1 and 6.2 respectively.

5 FINITE ELEMENT RESULTS

5.1 Untreated Curved Laminate

The stresses away from the free edges can be accurately modelled by simple analytical methods using a plane strain assumption. Close to the edges, however, this assumption does not hold and the stresses become highly complex, under the influence of a numerical singularity at the free edges. For example, there is an initial reduction followed by a sharp rise in direct through thickness stress near the edge, as illustrated in Fig. 8. This behaviour is caused physically by the discontinuity at the free edge and the differential strain of 0°, 90° and ±45° layers. Sharp changes near the free edge are also observed in through thickness shear stresses, τ_{13} and τ_{23}, within the interface layers. From Fig. 8, it is clear that analysing stresses at the mid-width, or by using plane strain assumptions, would grossly over predict the performance of curved laminate specimens. Instead, stresses must be assessed close to the edge, where failure is likely to initiate, in order to accurately predict CBS.

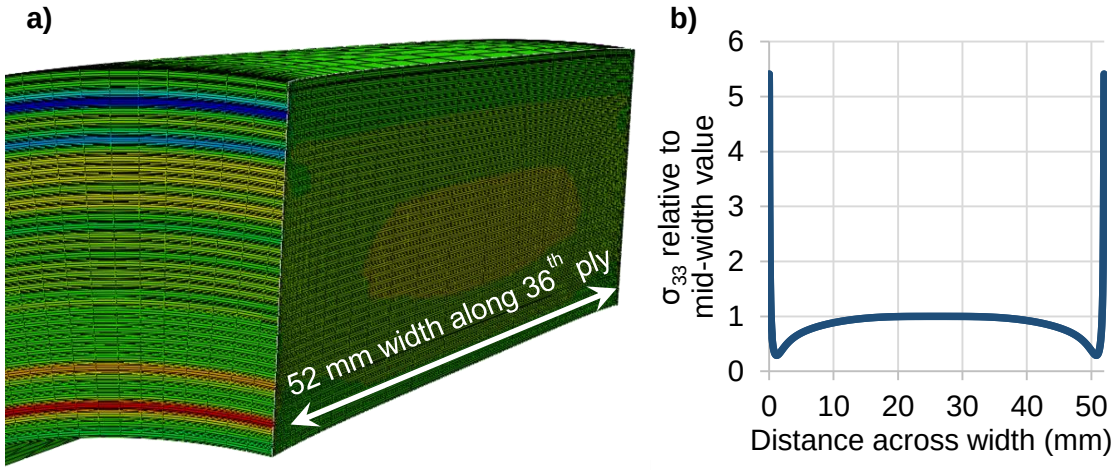

Figure 8 **a)** Curved laminate sectioned at the apex of the corner. Maximum tensile σ_{33} stress occurs at the edge of the 36th ply (4th from inner radius), which is a 0° ply. **b)** Plot of σ_{33} across the width of the 36th ply, with values normalised relative to the mid-width value. Near the free edges there is a sharp rise in σ_{33} stress in order to compensate for stresses normal to the free edge reducing to zero at the free edge.

5.1.1 Reliability of Model

The presence of a free edge creates a singularity in the Finite Element model, which significantly affects stress results obtained for the elements closest to the edge. Generally the first 2 elements adjacent to the free edge give unreliable results. Thereafter the effect of the free edge singularity rapidly dissipates, as evident in Fig. 8b. The influence of the singularity was investigated to determine when the predicted stress field can be considered reliable. Stresses were analysed at fixed physical distances of 60 μm and 500 μm away from the free edge. With different mesh refinements these physical distances could be represented by any number of finite elements (see for example Fig. 9). It was found that models that included 4 or more elements within the set distance showed negligible difference in their results, with less than 1% change in stress prediction, and were therefore assumed to have converged. Models with 3 elements within the distance gave a marginally different result (between 1-5%) and those with just 1 or 2 elements produced significantly different results (>5%). It was therefore determined that stress results at distances from the free edge similar to those considered (60-

500 μm) were only reliable if 4 or more elements exist between the free edge and the point of measurement. Moreover, stresses would never converge at the free edge regardless of mesh refinement, as a result of the singularity. This poses a problem for untreated curved laminate analysis since high stresses near the edge are likely to cause failure, yet it is difficult to reliably predict them. The authors seek to overcome this by modelling curved laminates with resin edge treatment, which is described in section 5.2.

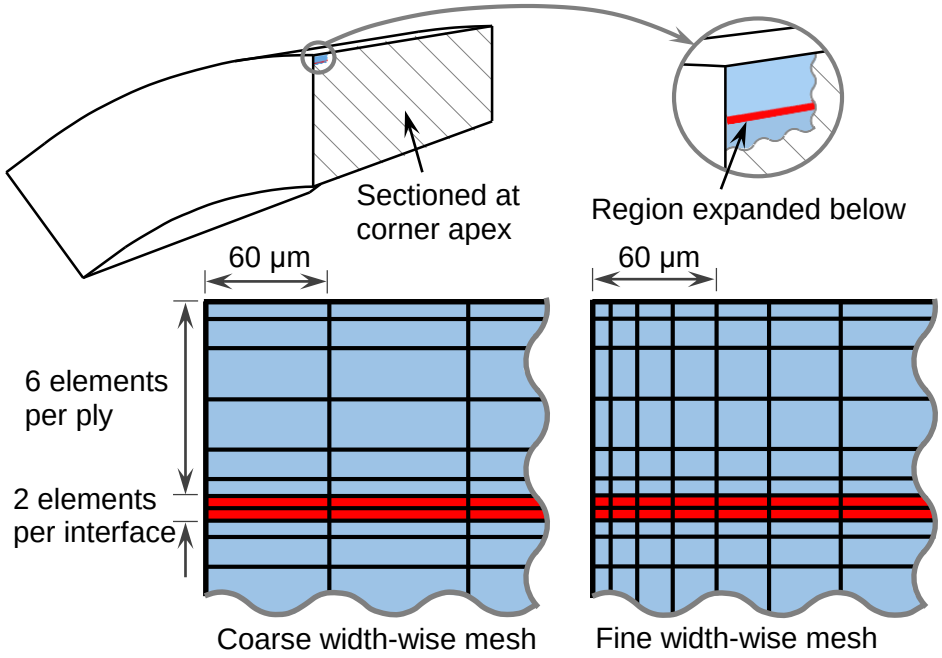

Figure 9 Illustration of a section of the FE model showing different mesh refinements.

5.1.2 Failure Location

The stresses near the free edge are complex, including inter-laminar shear and direct stress. Therefore a mixed mode failure criterion is more suitable than a maximum stress criterion. The strength of the laminates was assessed using a quadratic damage onset criterion, defined by Camanho et al [24] as

$$\sqrt{\left(\frac{\sigma_{33}^{+}}{s_{33}}\right)^2+\left(\frac{\tau_{13}}{s_{13}}\right)^2+\left(\frac{\tau_{23}}{s_{13}}\right)^2}=1 \quad , \tag{3}$$

with negative values of σ_{33} treated as zero. Using the untreated FE model, Fig. 10 shows the result of the LHS of Eq. (3), evaluated 4 elements (60 μm) away from the free edge on the apex of the corner, through the thickness (as per the fine mesh in Fig. 9). Note that the results for the resin edge treated laminate are also shown for comparison, which is discussed in section 5.2. In the case of the untreated laminate, failure is predicted to first occur near the inner radius within ply 36, where delamination was also observed during the test, along with other delaminations (see Fig. 3). The stress field at the peak in Fig. 10 is dominated by direct inter-laminar stress (σ_{33}). Note that failure, and hence CBS, cannot be predicted from Fig. 10 since the distance away from the edge (60 μm), at which stresses are assessed, is arbitrary. This distance is merely a consequence of evaluating stresses 4 elements away from the edge in accordance with reliability discussed in 5.1.1.

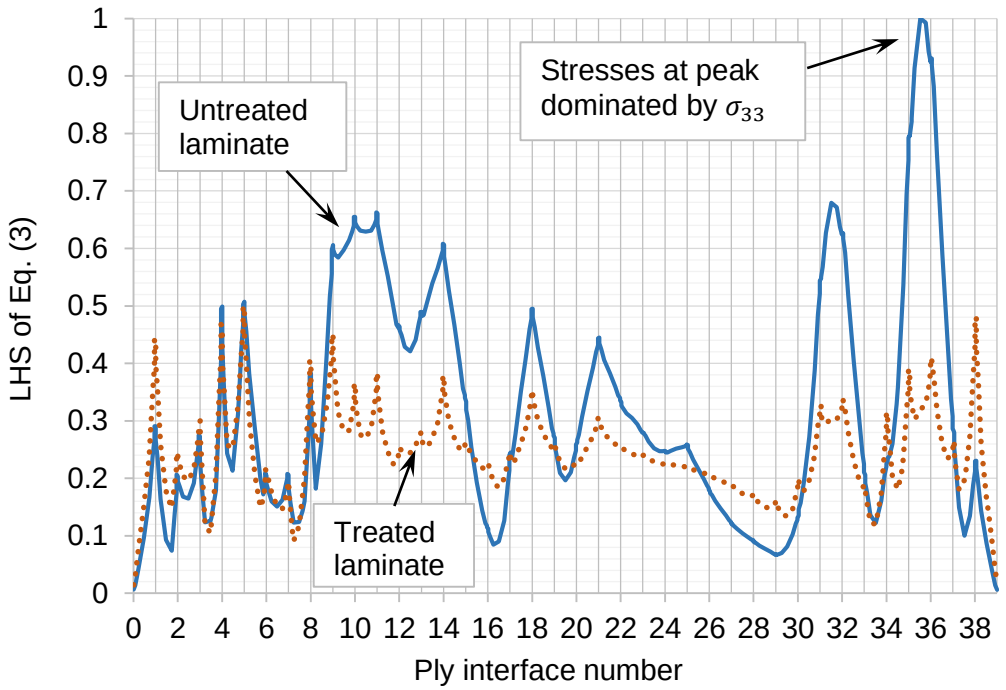

Figure 10 LHS of Eq. (3) evaluated at the corner apex, 4 elements (60 μm) away (width-wise) from the free edge for the untreated laminate and the resin edge-CFRP boundary for the treated laminate. This equates to the same location in the laminate for both models. Note that y-axis values are arbitrary but serve to show the difference between untreated and treated laminates with equal moment applied to both, indicating the effect of the resin edge treatment.

5.2 Curved Laminate with Resin Edge Treatment

The central CFRP section of the treated curved laminate was modelled with an identical mesh as for the untreated curved laminate. The resin edges (applied to the CFRP free edges) were meshed with 10 elements across their width (direction 1 in Fig. 1). Fidelity at the resin edge-CFRP boundary was increased using the single bias option in ABAQUS, with a bias ratio of 150. Through thickness and around the corner, the mesh seeding was identical to the central CFRP section. Figure 10 shows the effect the resin edge treatment has on stresses, by calculating the failure criterion at the same location within the laminate for both the untreated and treated laminates, with the same opening moment applied. The treatment generally suppresses stresses throughout the thickness, however the peaks tend to be dominated by shear rather than direct stress (see also Fig. 11) and in a few locations, particularly the inner- and outer-most interfaces, the failure criterion is increased by the resin edge treatment.

Unlike the untreated model, the presence of the resin edges in the treated model permits convergence at the CFRP edge. Therefore stresses can be taken at over very near the resin edge-CFRP boundary and are not arbitrary, unlike the untreated laminate stresses used to produce Fig. 10. Figure 11 shows the result of Eq. (3) evaluated one element (8 μm) away from the resin edge-CFRP boundary at the apex of the corner through thickness. This was done because stresses are ideally measured as close to the resin edge-CFRP boundary as possible, since this is where they are highest. However, taking them along the node line of the boundary would result in the averaging of stresses in the resin edge and CFRP section. From this analysis, a CBS of 8.25 kN/mm was predicted, giving a conservative result within 5% of the average test failure. Failure is predicted at ply interface 5, towards the outer radius, where test samples exhibited delamination, as well as in other locations (see Fig. 4a). It is noted however, that there are several peaks in Fig. 11 that are close to failure. The breakdown of stress values for the greatest 6 peaks are shown in Table 4. In contrast to the untreated

laminate failure criterion, interlaminar shear stress (either τ_{13} or τ_{23}) constitutes the largest stress and therefore dominates the failure criterion for the greatest 5 peaks.

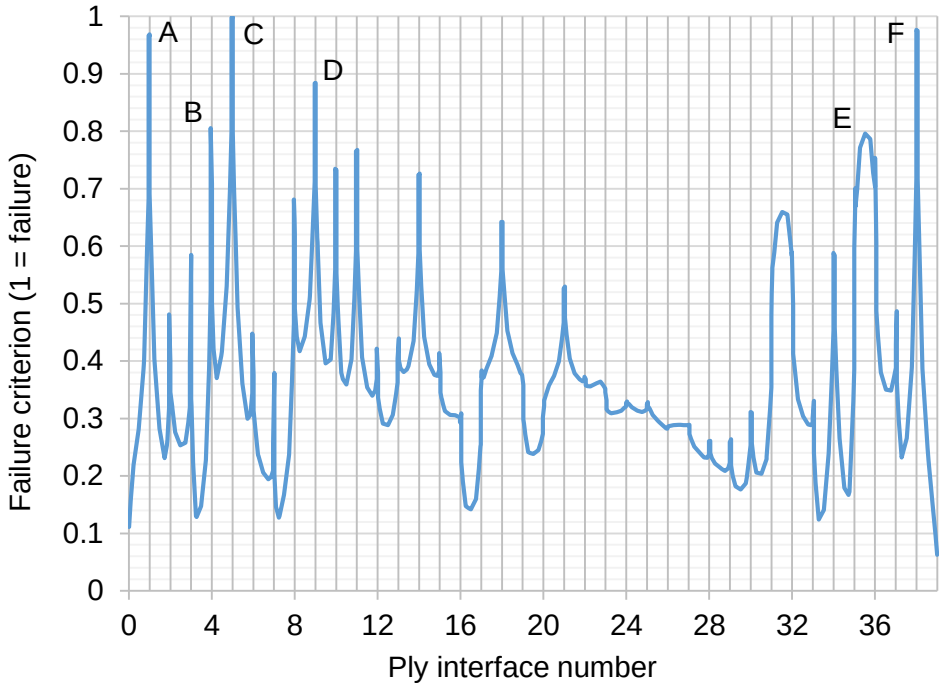

Figure 11 Failure criterion evaluated at the corner apex through the thickness of the treated laminate model. The value of applied running moment is 8.25 kNmm/mm. Stresses are evaluated one element (8 μm) away from the resin edge-CFRP boundary.

Peak	σ_{33}	τ_{13}	τ_{23}
A	18.3	2.0	-89.3
B	-12.9	-73.0	28.0
C	26.8	-13.7	-86.1
D	28.3	-17.7	-70.8
E	48.1	3.9	10.2
F	-16.6	6.7	-94.4

Table 4 Breakdown of stress components (in MPa) contributing to peak values in failure criterion in Fig. 11.

6 DISCUSSION

6.1 Comparison of Test Results and Analysis Predictions

Table 5 contains a summary of the test results and analysis predictions for curved laminate CBS. The free edge appears to have reduced strength by 21%, by comparing the untreated test average with CBS based on plane strain analysis. The resin edge treatment increases curved laminate CBS by 16% and the FE analysis gives a conservative prediction for this, within 5% of the average test failure.

Failure criteria	CBS (kNmm/mm)	
	No treatment	Edge treated
Test average	7.49 (18-37)	8.65 (1-37)
Plane strain	9.51 (23)	
FE Camanho	Un-converged	8.25 (5)

Table 5 Comparison between test results, plane strain and 3D FEA for curved laminates without and with resin edge treatment. Ply interface(s) of delamination is indicated in brackets and shown in Fig. 3 and Fig. 4 for two tests.

It is noted in section 4 that there is some uncertainty regarding ply and interface thicknesses, which also typically vary slightly within a laminate. A sensitivity study has been performed to investigate the impact that changing these thicknesses has on the CBS predicted by the FE analysis. Otherwise identical models of the resin edge treated laminates were created with ply (interface) thicknesses of 245 (10) μm, 240 (15) μm and 235 (20) μm. The model with thicknesses of 240 (15) μm ("baseline model") was used to product Fig. 11 and the FEA prediction for CBS in Table 5. The two models with extreme thicknesses either side of this predicted CBS to within ±5% of the baseline model result. The model with thicker interface layers of 20 μm predicted a CBS for the treated laminate of 8.60 kNmm/mm, which is within 1% of the test result. Modelling the interfaces as 10 μm thick, thinner than what has been seen in micrographs and found in the literature, is believed to be the worst case for determining the FE prediction accuracy. In this case the FE prediction is 10% below the test average. On the basis of this sensitivity study, the current FE modelling appears sufficient to predict CBS to

within at least 10% of the test value. However, with more accurate ply and interface thickness measurements, the method is likely to be significantly more accurate than this, as shown by the model with thicker interface layers.

Another possible source of error in the prediction of test CBS is failure of the resin edge treatment. The FE model was setup with an applied running moment equal to the average treated test CBS of 8.65 kNmm/mm. It was found that the maximum tensile stress in the resin edge caused by bending was 60 MPa. The EP1330LV datasheet quotes a UTS of 55 MPa. This would indicate that failure of the applied resin edge treatment is likely to have occurred first. At the point of failure during the test, it was observed that the resin edge shattered into many pieces and broke away from the CFRP (see Fig. 4), as well as multiple delaminations appearing in the CFRP, all within a fraction of a second. It was not possible to determine exactly which failure occurred first. If the resin edge fails, CFRP edge protection is lost and therefore the laminate is likely to fail simultaneously, since the untreated test CBS has already been exceeded at this point.

6.2 Analysis of the Free Edge Singularity

The singularity caused by the free edge makes FE modelling of the untreated curved laminates extremely challenging. In order to illustrate the effect, the plot in Fig. 12 has been generated by varying the mesh seeding across the width of the laminate (described previously in 4.1). The direct inter-laminar stress was measured one element away from the CFRP edge in the middle of the 36th ply, which is the 0° ply closest to the inner radius and is where maximum tensile σ_{33} is seen close to the CFRP edge. Note that the CFRP edge is the free edge for the untreated curved laminates and the boundary with the resin edge for the treated ones. By varying the width-wise mesh refinement, the size of the element at this edge was varied, as was the physical distance from the edge where stresses were being taken.

From Fig. 8b and Fig. 12 it appears that the untreated curved laminate stress value is tending towards infinity as it is measured closer to the free edge. This is because there can be no stress normal to the free edge. Other stresses, such as direct inter-laminar stress, become very large near the edge and infinite at the edge in order to compensate for this. In contrast, the treated curved laminate stress value converges to a finite value. This is because the presence of the resin edge allows for some stress normal to the CFRP edge, in turn preventing other stresses from becoming infinite. The result is that it is much more feasible to model the treated laminates to predict failure than the untreated ones, without a reliable method for determining how far from the free edge to evaluate untreated laminate stresses.

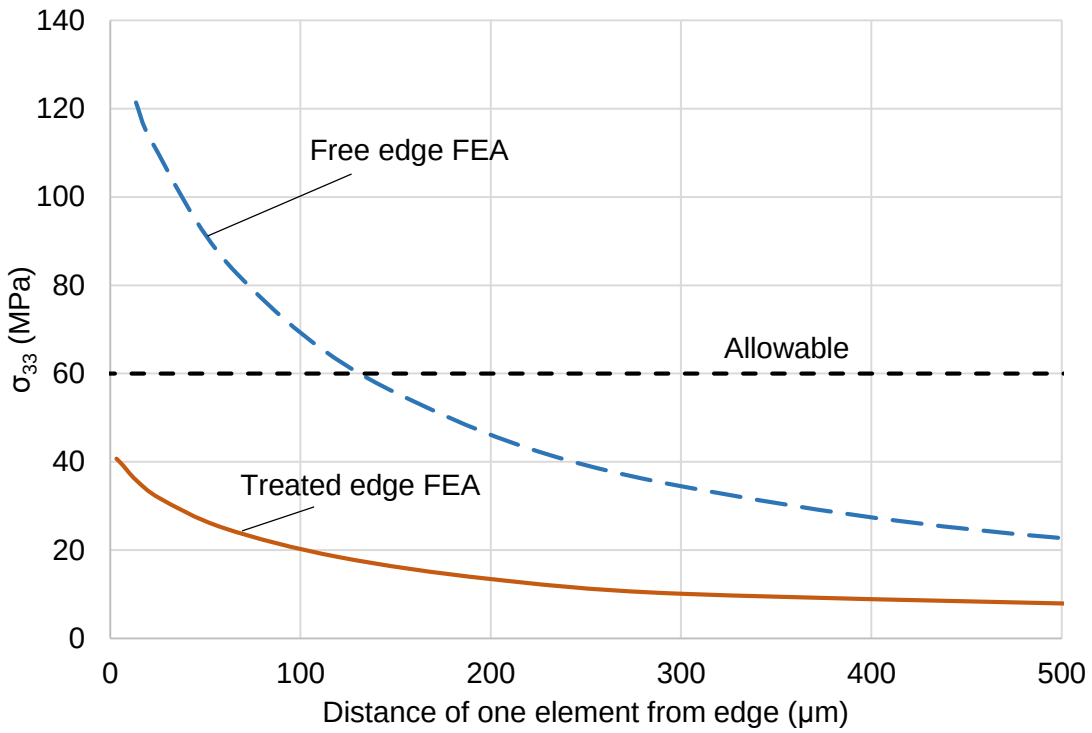

Figure 12 Tensile inter-laminar stress in ply 36, one element away from the CFRP edge for varying mesh refinements (width-wise). The untreated average test CBS of 7.49 kNmm/mm was applied. The σ_{33} allowable is also shown.

6.3 Effect of Resin Edge on Near-edge Interlaminar Stresses

The stress field in the vicinity of the free edge is highly complex, as is the way in which the resin edge treatment interacts with it. Interlaminar stresses τ_{13} and σ_{33} have been identified as critical components contributing towards failure near the free edge [23]. Comparisons between untreated and treated laminates of global interlaminar direct stress (σ_{33}) and interlaminar shear stress (τ_{13}) are shown in Fig. 13 and Fig. 14 respectively. The presence of a singularity in the untreated laminate dictates that stresses in the 1 direction (see Fig. 1) must be zero at the free edge. As a result other stresses become very large near the edge in order to compensate, as shown by σ_{33} stress tending towards infinity for the untreated laminate in Fig. 13. The presence of the resin edge treatment allows for a non-zero stress in the 1 direction at the CFRP edge, resulting in finite values for other stresses. This effect is shown in Fig. 13 for 3 different resin treatment moduli, which also shows higher modulus resin treatment suppresses σ_{33} further, near the CFRP edge. The modulus of the resin used for the edge treatment is therefore important. Figure 13 indicates that the peak σ_{33} stress for the 'high modulus' resin (E = 8.5 GPa) is approximately equal to the mid-width σ_{33} value, which is why a high modulus resin was used for the test sample treatment.

Although the resin treatment suppresses σ_{33} stress, this is not the case for all stresses. Since the stresses in the 1 direction no longer have to be zero at the CFRP edge, interlaminar shear stress, τ_{13}, can be significant in this vicinity. This is shown in Fig. 14 for 3 different resin treatment moduli, where the untreated laminate stress goes to zero at y/b = 1, with the stress in this vicinity increasing with increasing resin modulus. The significant reduction in σ_{33} and increase in τ_{13} near the CFRP edge causes a failure mode change for the edge treated laminates, which is why different delamination patterns are seen in Fig. 3 and Fig. 4a.

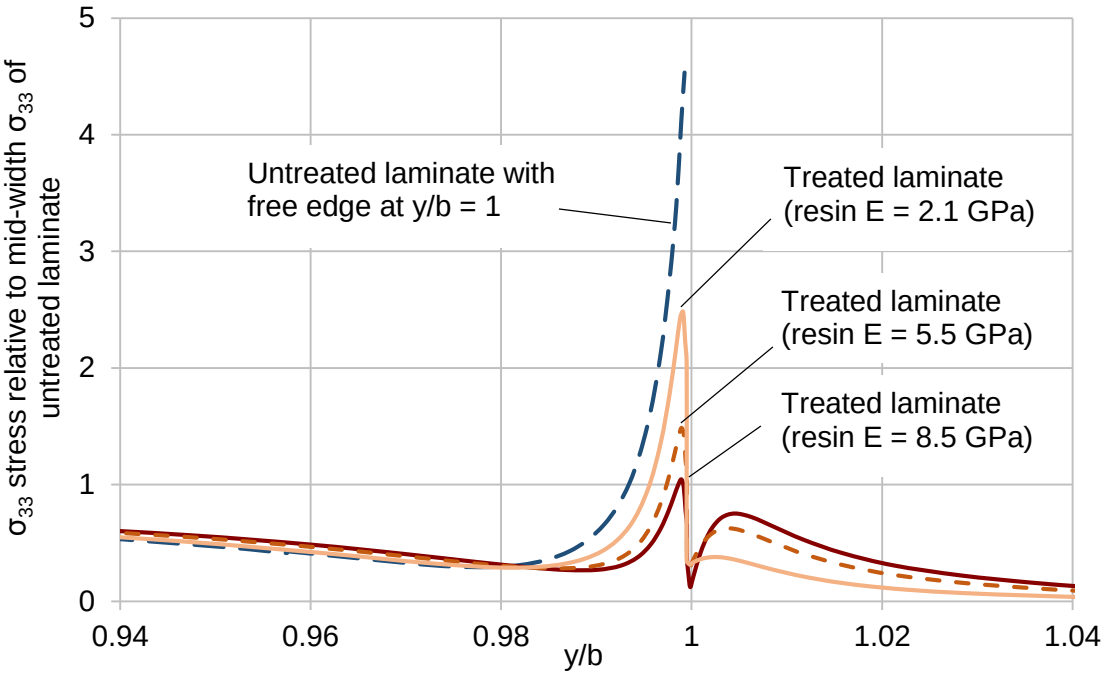

Figure 13 Global σ_{33} stress across the width of interface 36, between plies 36 and 37 (the 0/90 pair closest to the inner radius), normalised relative to mid-width σ_{33} of untreated laminate. Where b is the curved laminate width, y/b = 1 represents the free edge for the untreated laminate and the boundary between CFRP and resin edge for the treated laminate.

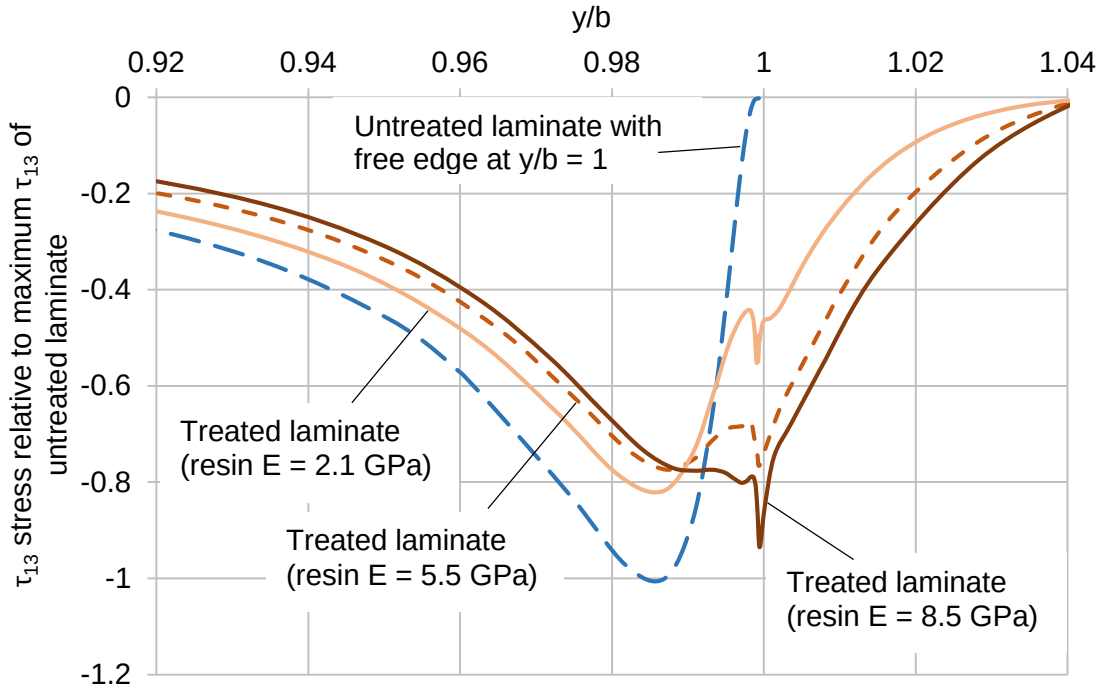

Figure 14 Global τ_{13} stress across the width of interface 38, normalised relative to maximum τ_{13} value in untreated laminate. Where b is the curved laminate width, y/b = 1 represents the free edge for the untreated laminate and the boundary between CFRP and resin edge for the treated laminate.

The use of edge caps [2-5] has also been shown to reduce interlaminar direct stress but not interlaminar shear stress. The caps consist of a C-shape that is clamped around the laminate at the free edge. This provides a means for development of none zero stresses normal to the free edge, similar to the effect of resin treatment in this work. Compared with the resin treatment however, edge caps are likely to provide greater support perpendicular to the free edge as a result of the clamping effect through thickness.

7 CONCLUSION

The free edges present in narrow test specimens reduce CBS by 21% compared with edgeless (or very wide) components according to plane-strain analysis. Current testing is therefore unreasonably conservative for wide parts, whereas the new approach provides confidence in a model-based method for assessing curved laminate strength. A new resin edge treatment reduced the edge effect and increased test specimen strength by 16%. Importantly, the addition of resin to the free edges removes the need for stresses normal to the edge to reduce to zero at the edge. This removes the singularity and prevents other stresses becoming infinite at the edge, which allows linear FE models to converge at the laminate edge. This paper shows that, with edge treatment, the initiation of failure can be successfully predicted to within 5% using linear FE analysis. The use of linear analysis vastly reduces computation time as compared with non-linear analysis, which will facilitate stochastic analysis of manufacturing induced imperfections and show the benefits of alternative laminate designs.

ACKNOWLEDGEMENTS

The authors would like to acknowledge the support of Jesper Ankersen (GKN Aerospace) and Vijay Sahadevan (GKN Aerospace). The fourth author is supported by a Royal Academy of Engineering / GKN Aerospace Research Chair.

REFERENCES

[1] American Society for Testing and Materials. ASTM D6415 / D6415M-06a, 2006. Standard test method for measuring the curved beam strength of a fiber-reinforced polymer-matrix composite.

[2] Kim RY. Prevention of free-edge delamination. In: Proceedings of the 28th National SAMPE Symposium and Exhibition, Azusa, 12-14 April 1983. p. 200-209.

[3] Heyliger PR, Reddy JN. Reduction of free edge stress concentration. J Appl Mech 1983;52:801-805.

[4] Howard WE, Gossard Jr T, Jones RM. Composite laminate free-edge reinforcement with U-shaped caps. Part I: Stress analysis. AIAA J 1989;27:610-616.

[5] Howard WE, Gossard Jr T, Jones RM. Composite laminate free-edge reinforcement with U-shaped caps. Part II: Theoretical-experimental correlation. AIAA J 1989;27:617-623.

[6] Vizzini AJ. Prevention of free-edge delamination via edge alteration. Paper no. 88-2258. In: Proceedings of the AIAA/ASME/ASCE/AHS 29th Structures, Structural Dynamics and Materials Conference, Williamsburg, April 18-20 1988. p. 365-370.

[7] Mignery LA, Tan TM, Sun CT. The use of stitching to suppress delamination in laminated composites. ASTM Symposium on delamination and debonding of materials. In: Proceedings of ASTM STP 876, American Society for Testing and Materials, Pittsburgh, 1985, p. 371-385.

[8] W.S. Chan, C. Rogers, S. Aker. Improvement of edge delamination strength of composite laminates using adhesive layers. Composite materials: testing and design (7th conference). In: Proceedings of ASTM STP 893, American Society for Testing and Materials, Philadelphia, 1986, p. 265-285.

[9] Chan WS, Rogers C, Cronkhite JD, Martin J. Delamination control of composite rotor hubs. J Am Helicopter Soc 1986;31(3):60-69.

[10] Mittelstedt C, Becker W. Free-edge effects in composite laminates. Appl Mech Rev 2007;60(5):217-245.

[11] Kant T, Swaminathan K. Estimation of transversely inter-laminar stresses in laminated composites – a selective review and survey of current developments. Compos Struct 2000;49(1):65-75.

[12] Andakhshideh A, Tahani M. Free-edge stress analysis of general rectangular composite laminates under bending, torsion and thermal loads. Eur J Mech A-Solids 2013;42:229-240.

[13] Helenon F, Wisnom MR, Hallet SR, Allegri G. An approach for dealing with high local stresses in finite element analyses. Compos Part A - Appl Sci Manuf 2010;41(9):1156-1163.

[14] Panigrahi SK, Pradhan B. Delamination damage analyses of FRP composite spar wingskin joints with modified elliptical adhesive load coupler profile. Appl Compos Mater 2008;15(4):189-205.

[15] Vidal P, Gallimard L, Polit O. Assessment of variable separation for finite element modelling of free edge for composite plates. Compos Struct 2015;123:19-29.

[16] Shiau L-C, Chue Y-H. Free edge stress reduction through fibre volume fraction variation. Compos Struct 1991;19(2):145-165.

[17] Dassault Systèmes Simulia Corp., Providence, USA. ABAQUS 6.12-3 User's Manual. 2012.

[18] Larberg Y, Akermo M. On the interply friction of different generations of carbon/epoxy prepreg systems. Compos Part A - Appl Sci Manuf 2011;42(9):1067-1074.

[19] HEXCEL Corporation. HexPly M21 curing epoxy matrix product data. 2010.

[20] HEXCEL Corporation. HexPly 8552 epoxy matrix product data. 2013.

[21] Berthe J, Deletombe E, Brieu M, Portemont G, Paulmier P. Dynamic characterization of CFRP composite materials – toward a pre-normative testing protocol – application to T700GC/M21 material. Procedia Eng 2014;80:165-182.

[22] Resinlab LLC. Technical data sheet EP1330 & EP1330LV. 2010.

[23] Esquej R, Castejon L, Lizaranzu M, Carrera M, Miravete A, Miralbes R. A new finite element approach applied to the free edge effect on composite materials. Compos Struct 2013;98:121-129.

[24] Camanho PP, Davila CG, De Moura MF. Numerical simulation of mixed-mode progressive delamination in composite materials. J Compos Mater 2003;37(16):1415-1438.